important to determine the subcellular compartment(s) (cytoplams, lysosomes, or other organelles) to which these types of vesicles can deliver their contents. We are currently evaluating these problems.

Acknowledgments

The technical assistances of C. M. Howard and Frank Tsakeres are acknowledged.

References

Ames, B., & Dubin, D. T. (1960) *J. Biol. Chem. 235*, 769.
Devreotes, P. N., & Fambrough, D. M. (1975) *J. Cell Biol. 65*, 335–358.
Gregoriadis, G. (1976a) *N. Engl. J. Med. 295*, 704–710.
Gregoriadis, G. (1976b) *N. Engl. J. Med. 295*, 765–770.
Gregoriadis, G., & Neerunjun, D. E. (1974) *Eur. J. Biochem. 47*, 179–185.
Gregoriadis, G., & Neerunjun, D. E. (1975) *Biochem. Biophys. Res. Commun. 65*, 537–544.
Huang, L., & Pagano, R. E. (1975) *J. Cell Biol. 67*, 38–48.
Juliano, R. L., & Stamp, D. (1975) *Biochem. Biophys. Res. Commun. 63*, 651–658.
Kennel, S. J. (1976) *J. Biol. Chem. 251*, 6197–6204.
Lowry, O. H., Rosebrough, N. J., Fall, A. L., & Randall, R. J. (1951) *J. Biol. Chem. 193*, 265–275.
Pagano, R. E., & Weinstein, J. N. (1978) *Annu. Rev. Biophys. Bioeng. 7*, 435–468.
Schieren, H., Weissmann, G., Seligman, M., & Coleman, P. (1978) *Biochem. Biophys. Res. Commun. 82*, 1160–1167.
Sonoda, S., & Schlamowitz, M. (1970) *Immunochemistry 7*, 885–898.
Weinstein, J. N., Blumenthal, R., Sharrow, S. O., & Henkart, P. A. (1978) *Biochim. Biophys. Acta 509*, 272–288.
Weissmann, G., Brand, A., & Franklin, E. C. (1974) *J. Clin. Invest. 53*, 536–543.
Weissmann, G., Bloomgarden, D., Kaplan, R., Cohen, C., Hoffstein, S., Collins, T., Gotlieb, A., & Nagle, D. (1975) *Proc. Natl. Acad. Sci. U.S.A. 72*, 88–92.

Phospholipid Lateral Phase Separation and the Partition of *cis*-Parinaric Acid and *trans*-Parinaric Acid among Aqueous, Solid Lipid, and Fluid Lipid Phases†

Larry A. Sklar,*,‡ George P. Miljanich,§ and Edward A. Dratz*

ABSTRACT: The partition of *cis*-parinaric acid (9,11,13,15-*cis*,*trans*,*trans*,*cis*-octadecatetraenoic acid, *cis*-PnA) and *trans*-parinaric acid (9,11,13,15-*all-trans*-octadecatetraenoic acid, *trans*-PnA) among aqueous, solid lipid, and fluid lipid phases has been measured by three spectroscopic parameters: absorption spectral shifts, fluorescence quantum yield, and fluorescence polarization. The solid lipid was dipalmitoylphosphatidylcholine (DPPC); the fluid lipid was palmitoyldocosahexaenoylphosphatidylcholine (PDPC). Mole fraction partition coefficients between lipid and water were determined by absorption spectroscopy to be, for *cis*-PnA, 5.3×10^5 with solid lipid and 9×10^5 with fluid lipid and, for *trans*-PnA, 5×10^6 with solid lipid and 1.7×10^6 with fluid lipid. Ratios of the solid to the fluid partition coefficients ($K_p^{s/f}$) are 0.6 ± 0.2 for *cis*-PnA and 3 ± 1 for *trans*-PnA. A phase diagram for codispersions of DPPC and PDPC has been constructed from the measurements of the temperature dependence of the fluorescence quantum yield and polarization of *cis*-PnA and *trans*-PnA and their methyl ester derivatives. A simple analysis based on the phase diagram and fluorescence data allows additional calculations of $K_p^{s/f}$'s which are determined to be 0.7 ± 0.2 for the cis probes and 4 ± 1 for the trans probes. The relative preference of *trans*-PnA for solid phase lipids and its enhanced quantum yield in solid phase lipids make it sensitive to a few percent solid. The trans probes provide evidence that structural order may persist in dispersions of these phospholipids 10 °C or more above their transition temperature. It is concluded that measurements of PnA fluorescence polarization vs. temperature are better suited than measurements of quantum yield vs. temperature for determining phospholipid phase separation.

Fluorescent probe molecules continue to contribute to the elucidation of membrane microstructure.[1] This work further develops *cis*-parinaric acid (*cis*-PnA,[2] 9,11,13,15-*cis*,*trans*,*trans*,*cis*-octadecatetraenoic acid) and *trans*-parinaric acid (*trans*-PnA, 9,11,13,15-*all-trans*-octadecatetraenoic acid) as fluorescent probes for biological membranes. In previous publications we have characterized the fluorescence response of these molecules to phospholipid phase transitions and lateral

† From the Division of Natural Sciences, University of California at Santa Cruz, Santa Cruz, California 95064. *Received August 1, 1978; revised manuscript received January 3, 1979.* This work was supported by the National Institutes of Health (Grant EY 00175 to E.A.D.). A preliminary account of this work was presented at the 1978 Biophysical Society Meeting.

‡ Present address: Division of Atherosclerosis and Lipoprotein Research, Department of Medicine, The Methodist Hospital and Baylor College of Medicine, Houston, TX 77030. L.A.S. is a Helen Hay Whitney Postdoctoral Fellow.

§ Present address: Department of Biochemistry and Biophysics, University of California, San Francisco, CA 94143. G.P.M. was supported by a student fellowship from the Abraham Silver Memorial Fund of the Fight for Sight, Inc., New York, NY.

[1] A recent review (Lee, 1977) contains leading references to the application of spectroscopic and other physical methods to phospholipid phase diagrams.

[2] Abbreviations used: *cis*-PnA, *cis*-parinaric acid; BHT, 2,6-di-*tert*-butyl-4-methylphenol; DPPC, dipalmitoylphosphatidylcholine; Hepes, *N*-(2-hydroxyethyl)piperazine-*N'*-ethanesulfonic acid; ME, methyl ester; *P*, fluorescence polarization ($I_{\parallel}/I_{\perp}$); PC, phosphatidylcholine; PDPC, 1-palmitoyl-2-docosahexaenoylphosphatidylcholine; *Q*, fluorescence quantum yield; TLC, thin-layer chromatography; *trans*-PnA, *trans*-parinaric acid.

0006-2960/79/0418-1707$01.00/0

phase separations, emphasized their structural similarity to common membrane acyl chains, and suggested that *trans*-PnA preferentially partitions into solid phase phospholipids, whereas *cis*-PnA partitions more equally between coexisting fluid and solid phospholipid phases (Sklar et al., 1975, 1977b).

We develop here a quantitative method to measure the partition of these probes between coexisting phases. The method requires several steps. We first construct (from measurements of the temperature dependence of PnA fluorescence quantum yield and polarization) the phase diagram of a binary phospholipid mixture which exhibits solid–solid immiscibility. Because we are particularly interested in the behavior of polyunsaturated phospholipids and their relevance to visual excitation, we have chosen to examine the phase diagram of dipalmitoylphosphatidylcholine (DPPC) and 1-palmitoyl-2-docosohexaenoylphosphatidylcholine (PDPC). The DPPC/PDPC phase diagram exhibits extensive solid phase immiscibility because the melting temperatures of the components differ by ~70 °C. Next, we calculate from the phase diagram the mole fraction of solid phase (χ_s) and fluid phase (χ_f) phospholipid. From the fluorescence measurements we can calculate the fraction of PnA in the solid phase (χ_s^p) and in the fluid phase (χ_f^p). The partition coefficient, $K_p^{s/f}$, which describes the distribution of PnA between coexisting solid (DPPC) and fluid (PDPC) phases is given by the relationship

$$K_p^{s/f} = (\chi_s^p/\chi_s)/(\chi_f^p/\chi_f) \quad (1)$$

In all, the properties of four probes, *cis*-PnA, *trans*-PnA, and their methyl ester derivatives, have been examined. The cis probes are found to exhibit a slight preference for the fluid phase, while the trans probes partition strongly into the solid phase. It is remarkable that the trans probes, due to an enhanced quantum yield and preferential partition, are sensitive to even a few percent solid phase. Understanding the probe partitioning allows us to faithfully reconstruct the temperature dependence of *cis*-PnA fluorescence polarization in PDPC/DPPC mixtures from measurements on the pure components.

We would like to point out that the analysis of fluorescence polarization developed here is independent of the exact nature of PnA motion in phospholipid bilayers. We have, therefore, chosen to analyze the simple fluorescence polarization ratio

$$P = I_{\parallel}/I_{\perp} \quad (2)$$

rather than the parameter normally associated with probe motion in membranes, the fluorescence anisotropy (Shinitzky et al., 1971; Lentz et al., 1976a,b):

$$r = (I_{\parallel} - I_{\perp})/(I_{\parallel} + 2I_{\perp}) \quad (3)$$

Methods described here are applied elsewhere to study lateral phase separation (Sklar et al., 1979) and the effects of calcium (L. A. Sklar, G. P. Miljanich, and E. A. Dratz, unpublished experiments) on the organization of bovine retinal rod outer segment membranes and phospholipids.

Materials and Methods

Conjugated Polyene Fatty Acids. *cis*-PnA and *trans*-PnA were prepared as previously described (Sklar et al., 1977b). Methyl ester derivatives of PnA were prepared with diazomethane and were the gifts of Dr. Robert Simoni (*trans*-PnA-ME) and Dr. Charles Berde (*cis*-PnA-ME). Silicic acid TLC developed with 9:1 hexane/diethyl ether and stained with iodine revealed no unconverted fatty acids; gas chromatography showed the isomeric purity to be 98%. Ethanolic stock solutions of all probes were used for addition to phospholipid dispersions.

Phospholipids. DPPC was obtained from Sigma and used without further purification. Purity was established by silicic acid TLC, developed in 65:25:5 chloroform/methanol/water. Gas chromatography of the fatty acid methyl esters, prepared by exposure to boron trichloride in methanol, indicated 98% purity with ~1% contamination from stearic acid. PDPC was prepared by the acylation of lysopalmitoyllecithin with docosahexaenoyl anhydride as described elsewhere (Miljanich et al., 1979). The product was analyzed to contain 96% PDPC and 4% didocosohexaenoylphosphatidylcholine.

Phospholipid Dispersions. One micromole of phospholipid, in chloroform solution, was deposited as a thin film on the walls of a Pyrex tube (12.5 × 1.6 cm with screw-top, Teflon-lined cap) by rotary evaporation under vacuum. The dried phospholipids were covered with 7.5 mL of buffer (pH 7.5, 115 mM NaCl, 10 mM Hepes, Ultrol grade obtained from Calbiochem). To ensure sample stability, care was taken to avoid oxidation damage to the probe and the lipids. BHT (1 BHT/500 PC) was added as an antioxidant as described previously (Sklar et al., 1977b), and the contents of the tube were vigorously bubbled with argon before the tube was capped. The capped mixtures were heated to 65 °C and the lipids were dispersed by shaking the tube in a vortex mixer at maximum speed for 2 × 15 s. This procedure provided dispersions of reproducible optical clarity (0.1 OD or less at the exciting wavelength) which did not sediment over the time course of the experiment. Phospholipid concentrations in the dispersions were verified by phosphate analysis (Chen et al., 1956).

Preparation of Samples for Fluorescence Measurements. Sample volumes were 2.5 mL, so that each dispersion provided two samples and a probe-free scattering blank. Conjugated polyene fatty acids were added as aliquots from stock solutions directly into sample cuvettes which were vigorously bubbled with a stream of argon at room temperature, except for *trans*-PnA-ME which was added at 50 °C to enhance the incorporation of probe into the lipids. Probe molecules were added at approximately 1 probe/166 PC, and the amount of probe in each sample was measured from the absorption spectrum of the dispersion compared to the scattering blank.

Absorption Spectroscopy. Spectra were recorded with a Cary 14 UV-vis scanning spectrophotometer equipped with a scattered transmission accessory.

Fluorescence Spectroscopy. Fluorescence polarization and quantum yield measurements were performed with a Hitachi Perkin-Elmer MPF 2A spectrofluorometer. A four-position variable temperature sample compartment was equipped with Glan-Taylor UV transmitting polarizers (8 and 15 mm clear aperture for excitation and emission, respectively) in rotatable mounts. The analyzing polarizer could be rotated 90° from outside the sample compartment from parallel to perpendicular orientation by a stopped sliding rod. The emission lens was covered by a $^3/_4$-in. aperture, reducing the solid angle viewed by the analyzing polarizer from ~60 to 38°. Stray light was reduced using ultraviolet band-pass filter UG 11 (Optical Industries) in the exciting beam and the MPF-2A 390-nm cutoff filter in the emission beam. All measurements employed identical instrumental settings, including 3- and 40-nm slit settings for excitation and emission, respectively. The excitation wavelengths for *cis*-PnA and *trans*-PnA were 325 and 320 nm in phospholipid dispersions. The emission wavelength was 410 nm. Absorption spectra of samples were recorded vs. scattering blanks before and after fluorescence mea-

Table I: Mole Fraction Lipid/Water Partition Coefficients[a]

	DPPC		PDPC		
	K_p	PnA bound/ PnA free[c]	K_p	PnA bound/ PnA free[c]	ROS membranes[b] K_p
cis-PnA	$(5.3 \pm 0.6) \times 10^5$	56/44	$(9.0 \pm 1.0) \times 10^5$	69/31	$(1.7 \pm 0.2) \times 10^6$ $(2.0 \pm 0.2) \times 10^6$ [d]
cis-PnA-ME[e]	$\sim 10^6$	71/29			$\sim 3 \times 10^6$
trans-PnA[f]	$(5.0 \pm 0.3) \times 10^6$	87/13	$(1.7 \pm 0.3) \times 10^6$	80/20	$(2.5 \pm 0.4) \times 10^6$
trans-PnA-ME[e,f]			$\sim 2 \times 10^6$	83/17	$\sim 5 \times 10^6$

[a] Partition coefficients were measured by ambient temperature (ca. 22 °C) observation of the absorption spectrum of solutions of PnA to which varying amounts of lipid had been added as described in the Materials and Methods section. It has been shown elsewhere (Sklar et al., 1977b) that equilibration of PnA in multilammellar vesicles occurs on the time scale of minutes in solid lipid and even faster in fluid lipid. All samples were incubated 15–30 min, some at 55 °C, prior to ambient spectral measurements. Heating had no effect on the final measurements. Error limits are estimated from uncertainties in spectroscopic parameters. [b] Retinal rod outer segment membranes, prepared according to Raubach et al. (1974). Assumes 75 phospholipids/rhodopsin. [c] Calculated according to eq 6 for 1.33×10^{-4} M lipid dispersion. [d] Determination at 1 °C. [e] Methyl ester values are estimates and may represent minimum values. [f] Dispersions of *trans*-PnA and *trans*-PnA-ME were prepared by slow injections of a dilute ethanolic stock solution in buffer, at 50 °C, while vigorously bubbling with argon.

surements. The scattering blanks were subjected to identical thermal cycles as the samples. The probe absorption in the sample typically changes less than 10% after continuous exposure to minimal UV illumination for periods of up to 2 h.

The polarizer alignment was verified with fluorescein in glycerol excited at its long wavelength absorption maximum. Defining polarization ratio, P, as $I_\parallel/I_\perp \times HH/HV$, we observe $P = 2.81 \pm 0.03$ for fluorescein in glycerol in good agreement with Chen & Bowman (1965).[3] $I_\parallel$ and $I_\perp$ refer to intensities emitted parallel and perpendicular to vertically polarized excitation and the factor HH/HV represents a correction for instrumental anisotropy (Azumi & McGlynn, 1962).

In measurements of the temperature dependence of fluorescence, temperature was varied at a rate not exceeding 1 °C/min by a circulating water bath and monitored by a thermocouple sealed in the sample cuvette within a few millimeters of the exciting beam. The output of the fluorometer was displayed on the x axis of a Varian XY recorder while the output of a Bailey digital thermometer was displayed on the y axis (5.5 °C/in.). $I_\parallel^{\text{sample}}$ and $I_\perp^{\text{sample}}$ were collected sequentially and virtually continuously, while $I_\parallel^{\text{blank}}$ and $I_\perp^{\text{blank}}$ were checked periodically. The polarization ratio is calculated from these data as

$$P = \frac{(I_\parallel^{\text{sample}} - I_\parallel^{\text{blank}}) \times HH/HV}{(I_\perp^{\text{sample}} - I_\perp^{\text{blank}})} = \frac{I_\parallel}{I_\perp} \quad (4)$$

where $HH/HV \approx 1.02$.

Fluorescence quantum yields, Q, were determined by comparing the total fluorescence intensity

$$I_{\text{tot}} = I_\parallel + 2I_\perp \quad (5)$$

of phospholipid dispersions containing PnA to the total fluorescence intensity of standard solutions of *cis*-PnA in ethanol at 25 °C where Q is known to be 0.020 (Sklar et al., 1977a). In order to calculate quantum yields for the probe in the lipid phase, however, the absorption spectrum of the probe in the dispersions had to be analyzed in terms of aqueous probe and lipid-bound probe contributions as described below. In addition, these determinations with *cis*-PnA in ethanol served as periodic standardization of any instrumental variability.

Partition of PnA Probes between Phospholipid and Aqueous Phases. We have previously used a direct binding assay to measure the partition of PnA probes between lipid and water (Sklar et al., 1977b). The mole fraction partition coefficient is defined by

$$K_p = \frac{\text{moles of bound PnA/moles of lipid}}{\text{moles of free PnA/moles of water}} \quad (6)$$

A spectroscopic procedure to determine water/lipid partition coefficients (Sklar et al., 1977b) relies on absorption spectral shifts. The spectrum of either *cis*-PnA or *trans*-PnA is red shifted 4–5 nm when PnA is moved from buffer to a phospholipid bilayer (Figure 1A). K_p is determined according to eq 7 by establishing from the absorption spectrum the lipid

$$K_p = (\text{moles of water})/(\text{moles of lipid}) \quad (7)$$

concentration at which free and bound PnA species are equal (Sklar et al., 1977b).

The determination of K_p for PnA-ME is complicated because the spectral shifts associated with PnA-ME binding to lipid are less distinct (Figure 1B). K_p is estimated from changes in the extinction coefficient and spectral broadening in this case.

Calculation of the Quantum Yield of PnA Probes in Phospholipid Dispersions. The quantum yield, Q, may be calculated from the intensity, I_{tot}, as derived from experimental data by eq 5. Under practical experimental conditions (see Discussion) a significant fraction of the probe molecules is in the aqueous phase (see Table I). In order to calculate Q of the lipid-bound probe as a function of temperature, we must know the proportion of free and bound probe and the con-

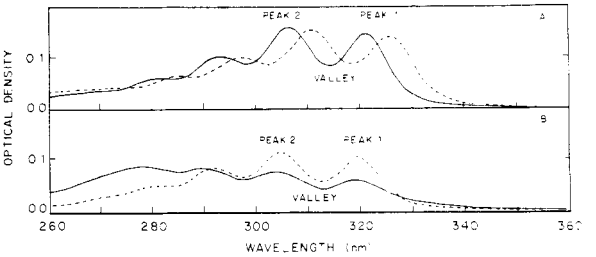

FIGURE 1: Absorption spectra of PnA probes in buffer and lipid dispersions. (A) *cis*-PnA ($\sim 3 \times 10^{-6}$ M) in buffer (solid line) and in the presence of 1 mM DPPC. (B) *trans*-PnA ME ($\sim 2 \times 10^{-6}$ M) in buffer (solid line) and in the presence of ~ 0.3 mM PDPC. The wavelength differences between aqueous and lipid-bound probe seen in A are related to environmental polarizability (Sklar et al., 1977a,b). The similarity in peak position of *trans*-PnA-ME in buffer and lipid suggests a similarity of environments; the elevation of absorption in the 280-nm region in buffer probably reflects excitonic interactions between neighboring probe molecules. These results suggest that ME derivatives form aggregates or "droplets" in water.

[3] Usually polarization is defined by $p = (I_\parallel - I_\perp)/(I_\parallel + I_\perp)$. For fluorescein in glycerol, Chen & Bowman (1965) obtain $p = 0.477$ which converts to $P = 2.83$ for $P = I_\parallel/I_\perp$.

tribution of each to the absorption spectrum. Two simplifying assumptions are utilized.

A. At temperatures away from the transition temperature, K_p is assumed to be temperature independent. [K_p is, in reality, probably a slowly varying function of temperature (Table I, and Simon et al., 1977).]

B. We approximate the partition coefficient of a lipid mixture by a single value, K_p^{mix}, for all temperatures

$$K_p^{mix} \equiv K_p^{solid}\chi^{solid} + K_p^{fluid}\chi^{fluid} \approx K_p^{DPPC}\chi^{DPPC} + K_p^{PDPC}\chi^{PDPC} \quad (8)$$

where $\chi^{DPPC} + \chi^{PDPC} = 1$ and represent the mole fractions of DPPC and PDPC. K_p^{DPPC} is for solid DPPC and K_p^{PDPC} is for fluid PDPC (Table I). This expression is appropriate at low temperatures where nearly pure DPPC and PDPC are laterally separated. If the fluid phase contains considerable DPPC (i.e., at high temperature), this latter expression tends to become a poorer approximation. However, $K_p^{s/f}$ values are calculated (see below) from eq 8 only at low temperatures where little DPPC is present in the fluid phase. In addition, this expression is adequate for calculations of the quantum yield of probe in the lipid even at high temperatures because nearly all the *trans*-PnA is bound in both fluid and solid phases even though there are large differences in K_p (Table I), and for *cis*-PnA, the K_p values for fluid and solid phase lipids are quite similar. Under our particular experimental conditions there is only a small change in the fraction of probe bound going from fluid to solid phase so eq 8 will be an adequate approximation.[4]

The relative contribution of free and bound species to the optical density, OD, at the exciting wavelength depends upon their relative extinction coefficient, ϵ, and concentrations.[5] On the basis of Figure 1, $\epsilon_{free}/\epsilon_{bound} \sim 0.6$ for both fatty acid and methyl ester probes at 320 nm (trans) and 325 nm (cis). Combining eq 6 with Beer's law, we conclude that

$$\frac{OD_{bound}}{OD_{free}} = \frac{\epsilon_{bound}}{\epsilon_{free}} \times K_p \times \frac{\text{moles of lipid}}{\text{moles of water}} = (0.6)^{-1}K_p \frac{\text{moles of lipid}}{\text{moles of water}} \quad (9)$$

Since K_p is constant for a given lipid system, the OD_{bound}/OD_{free} ratio is a constant, α, independent of probe concentration at a fixed lipid concentration. OD_{total} is determined spectrophotometrically for each sample. Substituting $OD_{free} = OD_{tot} - OD_{bound}$ into eq 9 and rearranging yields

$$OD_{bound} = (OD_{tot}\alpha)/(1 + \alpha) \quad (10)$$

Since the quantum yield of the free species is essentially zero, $I_{tot} = I_{tot}^{bound}$ and the quantum yield, Q, of bound probe is calculated as

$$Q = \frac{I_{tot}^{bound}/OD_{bound}}{I_{tot}^{EtOH}/OD_{EtOH}} \times 0.02 \quad (11)$$

where I_{tot}^{EtOH} and OD_{EtOH} refer to measurements on a stock solution of *cis*-PnA in ethanol, at 25 °C, with excitation at 320 nm. I_{tot}^{EtOH} is defined as in eq 5 and the factor 0.02 is Q_{EtOH} (Sklar et al., 1977a).

We define the quantities $Q_\parallel$ and $Q_\perp$, "partial quantum yields", such that

$$Q = Q_\parallel + 2Q_\perp \quad (12)$$

where the fluorescence polarization, P, is then

$$P = Q_\parallel/Q_\perp \quad (13)$$

Calculation of the Partition of PnA Probes between Coexisting Solid Lipid and Fluid Lipid Phases. The solid–fluid partition coefficient of a probe, $K_p^{s/f}$, is as previously defined by eq 1. We define $\chi_s^p + \chi_f^p = 1$ to represent all of the bound and fluorescent probe. χ_s and χ_f are the fractions of solid and fluid phase and may be calculated from the phase diagram (as constructed in the Results section). In order to calculate $K_p^{s/f}$ we must evaluate χ_s^p and χ_f^p. Below, we describe two methods based on measurements of Q and P.

The observed quantum yield at a given temperature, Q^{mix}, is only due to bound probe but may emanate from probe molecules in distinct lipid environments. Q^{mix} is a weighted average of the probe quantum yield in each environment multiplied by the fraction of probe molecules in each environment

$$Q^{mix} = Q^s\chi_s^p + Q^f\chi_f^p \quad (14)$$

where Q^s and Q^f are the quantum yields in pure solid (DPPC) and pure fluid (PDPC), respectively. Since

$$\chi_s^p = 1 - \chi_f^p \text{ and } \chi_f^p = 1 - \chi_s^p \quad (15)$$

substitution into eq 14 and rearrangement gives

$$\chi_f^p = (Q^{mix} - Q^s)/(Q^f - Q^s) \quad (16)$$

and

$$\chi_s^p = (Q^{mix} - Q^f)/(Q^s - Q^f) \quad (17)$$

Substitution of eq 16 and 17 into eq 1 yields

$$K_p^{s/f} = \frac{(Q^{mix} - Q^f)\chi_f}{(Q^s - Q^{mix})\chi_s} \quad (18)$$

In an analogous fashion, the partial quantum yields (which are measured experimentally) obey relationships of the form of eq 14 so that the polarization ratio, P, is then of the form

$$P = \frac{Q_\parallel^{mix}}{Q_\perp^{mix}} = \frac{Q_\parallel^s\chi_s^p + Q_\parallel^f\chi_f^p}{Q_\perp^s\chi_s^p + Q_\perp^f\chi_f^p} \quad (19)$$

or

$$P(Q_\perp^s\chi_s^p + Q_\perp^f\chi_f^p) = Q_\parallel^s\chi_s^p + Q_\parallel^f\chi_f^p \quad (20)$$

where $Q_\parallel^s$ and $Q_\perp^s$ are the partial quantum yields in pure solid (DPPC) and $Q_\parallel^f$ and $Q_\perp^f$ are the partial quantum yields in pure fluid (PDPC).

Treating eq 20 in a fashion analogous to the treatment of eq 14 yields

$$K_p^{s/f} = \frac{(PQ_\perp^f - Q_\parallel^f)\chi_f}{(Q_\parallel^s - PQ_\perp^s)\chi_s} \quad (21)$$

A comparable equation can be obtained using Weber's law for the additivity of polarization anisotropy (Weber, 1952) as described by Lentz et al. (1976b).[6]

[4] In this case, fluorescence intensities, normalized for total probe absorption in different samples, could be substituted for quantum yields in the derivation which follows.

[5] The extinction coefficients of PnA in fluid and solid lipids are similar at the excitation wavelength.

[6] Weber's law is given by the relationship $rQ = \sum_i r_iQ_i\chi_i$, where r and Q refer to the measured anisotropy and quantum yield in a mixture in which individual fluorescent species (i) have anisotropy (r_i) and quantum yield (Q_i) and comprise the mole fraction χ_i. Since our anisotropies (eq 3) and quantum yields (eq 13) are calculated from the same measurements, Weber's law reduces to $(Q_\parallel - Q_\perp) = \sum_i(Q_\parallel^i - Q_\perp^i)\chi_i$, which is similar in form to eq 14.

Results

Phospholipid/Water Partition Coefficients of PnA Probes. Partition coefficients, K_p, of PnA probes between phospholipid and aqueous phases were determined by examining changes in the absorption spectrum of PnA in the presence of varying amounts of phospholipid as described in the Materials and Methods section. Results are summarized in Table I. K_p values for PnA probes in DPPC, PDPC, and a biological membrane where these phospholipids occur (the bovine retinal rod outer segment) range from 5×10^5 to 5×10^6. We observe that this spectroscopic assay yields a partition coefficient for *cis*-PnA in DPPC ($5.3 \pm 0.6 \times 10^5$) that is similar to a previous direct binding assay ($4.7 \pm 0.7 \times 10^5$) (Sklar et al., 1977b). Although *cis*-PnA and *trans*-PnA partition in a relatively similar fashion in fluid PDPC, *cis*-PnA is relatively excluded by solid DPPC and *trans*-PnA is relatively included. The K_p values for solid phase differ by a factor of 10 for the two probes. K_p values for the retinal rod outer segment, a highly unsaturated biological membrane, are of similar magnitude to those of PDPC and apparently are not strongly temperature dependent. K_p values for the ME probes are estimated to be somewhat greater than those for the fatty acids.

We note that the solid/fluid partition coefficient ($K_p^{s/f}$) may be determined from the ratio K_p^{DPPC}/K_p^{PDPC}. The data in Table I indicate that $K_p^{s/f}$ is 0.6 ± 0.2 for *cis*-PnA and 2.9 ± 0.7 for *trans*-PnA. These results are consistent with our contention that *trans*-PnA preferentially partitions into the solid lipid phase, whereas *cis*-PnA distributes more equally between coexisting phases with slight preference for fluid phases.

Also included in Table I are calculated values of the fractions of the probe bound/probe free, based on eq 6 for the lipid concentration used in the fluorescence studies which follow. Note that under our typical conditions a threefold reduction in K_p (from 5×10^6 to 1.7×10^6) changes the fraction bound by only 10%, whereas a further twofold reduction (from 9×10^5 to 5×10^5) reduces the amount bound by about 25%. For this reason, small temperature-dependent variation of K_p, over a temperature range away from structural changes, will have only a small effect on the amount of probe bound (as assumed in the Materials and Methods section) and the calculated quantum yields.

Polarization of Fluorescence of PnA Probes in DPPC/PDPC Mixtures. The polarization ratio P, defined as $I_\parallel/I_\perp$, from eq 4, is plotted in Figure 2 as a function of temperature for the PnA probes in codispersions of various mixtures of DPPC and PDPC. In pure DPPC, *cis*-PnA (Figure 2A, 100% curve) and *cis*-PnA-ME (Figure 2B, 100% curve) show sharp increases in polarization centered at about 41 °C and 1–2 °C in width. Above and below this temperature range, the polarization ratio is weakly dependent on temperature. As the fraction of DPPC is reduced, the temperature at which the polarization begins to increase is lowered (as indicated by the arrows) and the final polarization level at lower temperatures is substantially reduced. We associate the temperature region above the arrows with complete formation of fluid lipid phase and the region beginning with the arrow and below as the onset of solid phase formation ("lateral phase separation") (Shimshick & McConnell, 1973); the final leveling off of the polarization, as the temperature is decreased, is taken to be the completion of the lateral phase separation. The response of *trans*-PnA or *trans*-PnA-ME (Figure 2C,D) to these phenomena is considerably different.

Whereas *cis*-PnA barely detects 10% DPPC, both trans probes readily detect the formation of solid phase in the

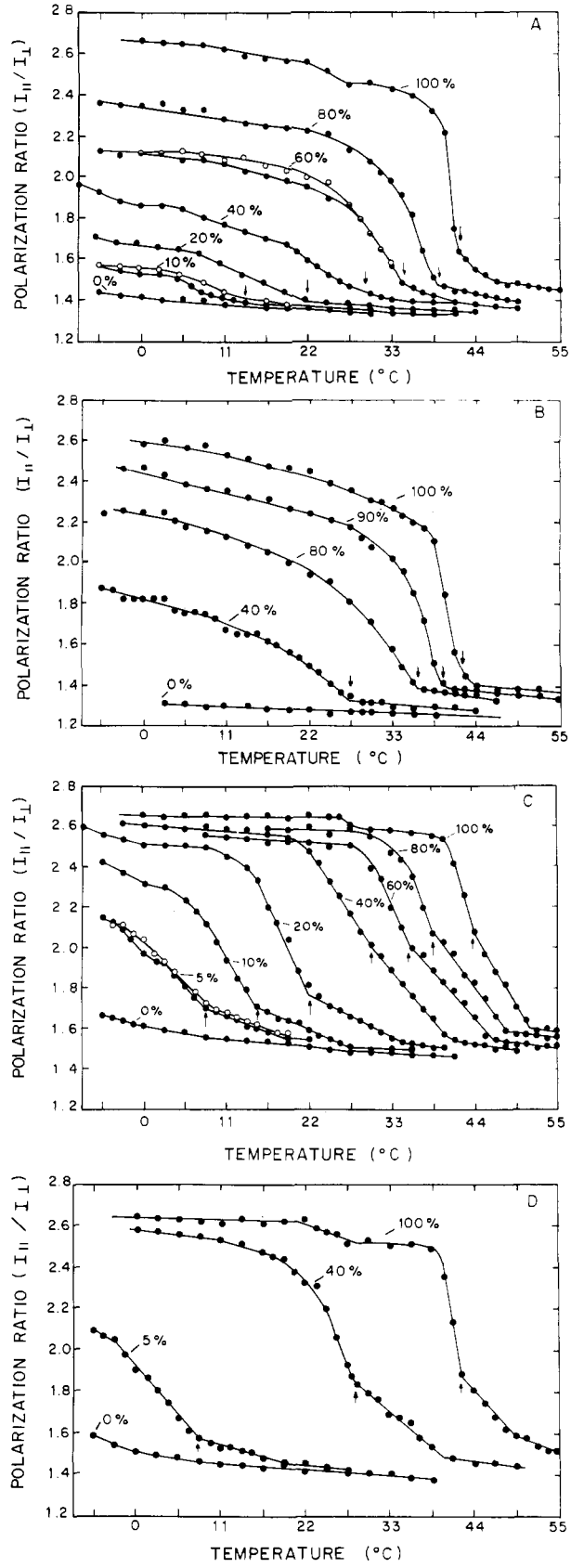

FIGURE 2: Polarization of fluorescence of PnA probes in DPPC/PDPC mixtures vs. temperature. (A) *cis*-PnA, (B) *cis*-PnA-ME, (C) *trans*-PnA, (D) *trans*-PnA ME. The numbers above the curves represent the percentage of DPPC. Data is plotted at 2.75 or 1.375 °C intervals and the temperature scale is calibrated in 11 °C intervals. For explanation of temperature interval see Materials and Methods section. Data shown is for cooling curves (●); representative heating curves are shown (○).

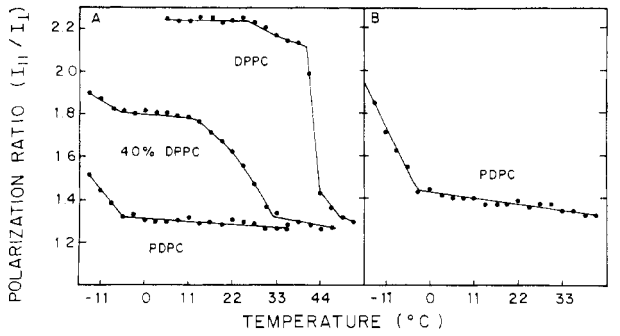

FIGURE 3: Low-temperature polarization of fluorescence of *cis*-PnA (A) and *trans*-PnA (B) in DPPC and PDPC. Samples were essentially as in Figure 2 except they contained 30% glycerol. For the data in this figure only, the fluorometer was equipped with a 2-in. UV 105 WRMR Polacoat sheet polarizer mounted on quartz as the emission polarizer; the emission aperature was omitted (see Materials and Methods section). The fluorescein in glycerol calibration of this setup gave a polarization ratio of 2.3.

mixture containing only 5% DPPC. Whereas intermediate polarization ratios are observed by the cis probes for mixtures, the polarization ratio of the trans probes at low temperatures in the presence of more than 40% DPPC approaches the values observed in 100% DPPC. At temperatures above the arrows, the polarization ratio of the cis probes is rather flat, but at comparable temperatures the trans probes exhibit "tails" which in the case of 100% DPPC persist nearly 10 °C above the transition temperature. Similarly, below 0 °C some of the polarization curves exhibit an upward curvature which is seen more clearly in Figure 3. The low-temperature curvature may represent PDPC clustering in the fluid phase.

Quantum Yield of PnA Probes in DPPC/PDPC Mixtures. Fluorescence quantum yields Q, calculated according to the scheme in the Materials and Methods section, of PnA probes in DPPC/PDPC dispersions are plotted as log Q vs. $1/T$ in Figure 4. The rationale for this form of the plot is discussed elsewhere (Sklar et al., 1977b) where we indicated that completely solid and completely fluid regions are represented by nearly linear and approximately parallel segments in such a plot. However, phase transition or lateral phase separation is marked by upward deviations from the fluid slope (at the high-temperature onset) and the approximate resumption of linearity (at the low-temperature completion) (Sklar et al., 1977b). The increasing quantum yield in the transition region is associated with the appearance of a long-lifetime, high quantum yield probe species characteristic of the solid phase (Sklar et al., 1977b). The quantum yields in Figure 4 are calculated from the same measurements used in calculating the polarization presented in Figure 2. The response of the probes to phospholipid structural reorganization analyzed by either method is directly comparable in most respects. As shown in Figure 4, the trans probes detect structural changes in the presence of 5% DPPC, but do not readily distinguish between 60 and 100% DPPC on the basis of the final low-temperature quantum yields. The *trans*-PnA curves in Figure 4 exhibit "tails" at temperatures above the arrows (placed as in Figure 2). In contrast, the cis probes are weakly responsive to structural changes in the presence of less than 40% DPPC and detect no order at temperatures where trans probe "tails" are observed. At low temperatures, the observed quantum yield of the cis probe is distinctive for all of the DPPC/PDPC mixtures. Similar quantum yield differences between the cis probes and the trans probes are also observed with single temperature measurements of mixtures of varying proportion of pure DPPC liposomes with pure PDPC or egg yolk liposomes (not shown).[7] As will be discussed, all these differences

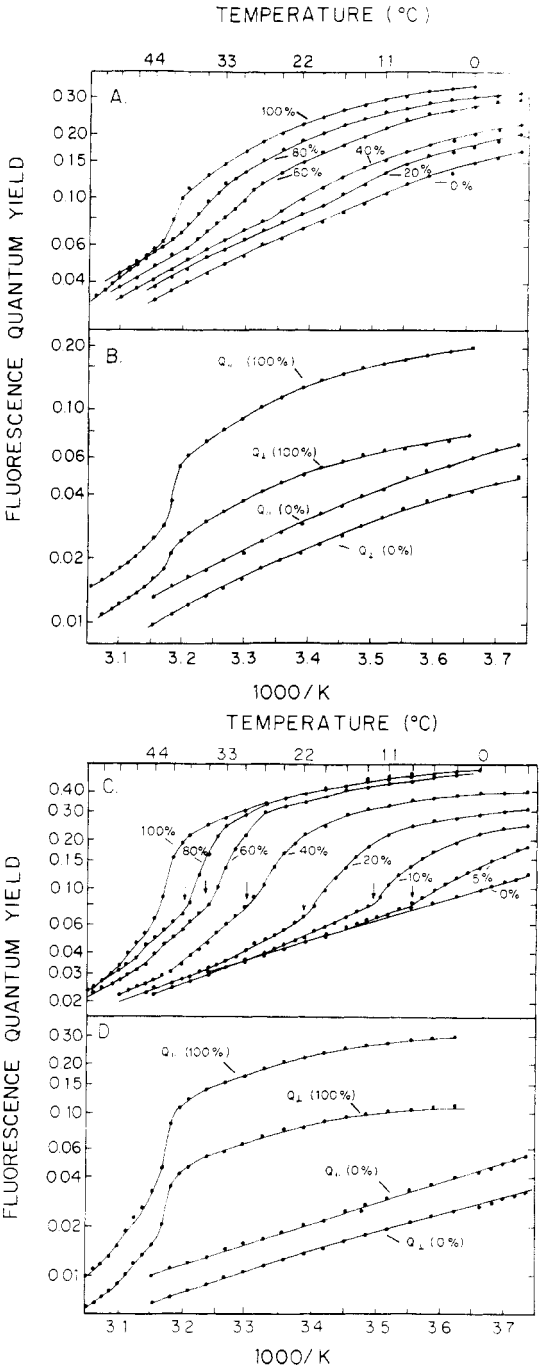

FIGURE 4: Log fluorescence quantum yield vs. (absolute temperature)$^{-1}$ of PnA probes in DPPC/PDPC mixtures. Total quantum yields are shown for *cis*-PnA (A) and *trans*-PnA (C). Partial quantum yields are shown for *cis*-PnA (B) and *trans*-PnA (D). Percents refer to DPPC. Calculation of partial quantum yields, $Q_{\parallel}$ and $Q_{\perp}$, is explained in the Materials and Methods section. The small corrections to quantum yield of sample turbidity are neglected.

between the sensitivity of the cis probes and trans probes to solid lipid are consistent with their respective solid lipid/fluid lipid partition coefficients, $K_p^{s/f}$.

The partial quantum yields $Q_{\parallel}$ and $Q_{\perp}$, defined in eq 12, are plotted in Figure 4B,D for the *cis*-PnA and *trans*-PnA in

[7] A preliminary investigation of the partition of PnA probes between egg yolk PC liposomes and DPPC liposomes was undertaken at a single temperature (10 °C) using the polarization of fluorescence. Results are very similar to those of Figure 6. The $K_p^{s/f}$ values were found to be >2 (*trans*-PnA and *trans*-PnA-ME) and <1 (*cis*-PnA and *cis*-PnA-ME). Several hours may be required to establish an equilibrium distribution of PnA-ME probes between the liposome populations at this temperature.

Table II: Analysis of DPPC/PDPC Phase Diagram[a]

temp (°C)	% solid phase							composition fluid (% PDPC)
	(5.0)[b]	(10.0)	(20.0)	(40.0)	(60.0)	(80.0)	(90.0)	
−5.5	4.0	9.1	19.2	39.4	59.6	79.8	89.8	99
0.0	3.1	8.2	18.4	38.8	59.2	79.6	89.7	98
5.5	1.3	6.5	16.9	37.7	58.4	79.2	89.6	96
11.0	0.0	3.7	14.4	35.8	57.2	78.6	89.3	92
16.5		0.0	9.1	31.8	54.5	77.2	88.6	88
22.0			0.6	26.4	50.3	75.2	87.6	80
27.5			0.0	0.0	41.6	70.8	85.4	68
33.0					20.0	60.0	80.0	50
38.5					0.0	0.0	42.9	17.5
44.0							0.0	

[a] The percent solid phase was calculated for various DPPC/PDPC mixtures from Figure 5 (using solidus curve S_2) according to the lever rule (Moore, 1962). The solid phase is pure DPPC and the fluid phase composition is calculated from the fluidus curve (Figure 5). The temperature interval (5.5 °C) is explained in the Materials and Methods section (Fluorescence Spectroscopy). [b] Numbers in parentheses represent percent DPPC in mixture of DPPC and PDPC.

pure DPPC and PDPC. In all quantum yield measurements the behavior of the methyl ester probes (data not shown) is similar to that of the free fatty acids except that the quantum yield values are 10–20% lower everywhere.

DPPC/PDPC Phase Diagram. A phase diagram for the binary mixture DPPC and PDPC is shown in Figure 5. The fluidus temperatures, curve F, are those corresponding to the arrows in Figure 2 and represent what we believe to be the onset of solid phase formation. Changes in the fluorescence parameters of the trans probes at temperatures higher than the arrows may be related to the presence of lipid clusters in the fluid phase (see Discussion).

The solidus curve represents the temperature below which the lipid mixture is 100% solid. Our criterion that a lipid mixture is 100% solid is that *cis*-PnA approaches its limiting solid phase polarization value. We have verified that the polarization ratio of *cis*-PnA approaches its solid phase value when a dispersion of PDPC (in propanediol/water) is cooled to −25 to −30 °C (data not shown). Since these low temperatures are not readily accessible, we examined mixtures containing high percentages of DPPC with the cis probes to see if we could detect residual fluid phase at low temperatures. The 90% DPPC mixture (Figure 2B) appears to contain some residual fluid phase down to at least −5 °C. Under the conditions described in Figure 3, an 80% DPPC mixture (data not shown) is not 100% solid at −16.5 °C. The upper limit to the solidus curve, inferred from these measurements, is represented by S_1 in Figure 5. A solidus curve represented by S_2 is expected in phase diagrams of binary lipid mixtures where there is both a large difference in acyl chain length and transition temperature between phospholipid species (Mabrey & Sturtevant, 1976; Wu & McConnell, 1975; Jacobs et al., 1977). Solidus curve 2 represents a limiting case of complete solid phase immiscibility for the DPPC/PDPC mixture. Differential scanning calorimetry of dioleyol PC and DPPC mixtures (Phillips et al., 1970) demonstrates considerable solid phase immiscibility. Dispersions of pure DOPC have a phase transition centered at −22 °C (Phillips et al., 1970) so that its behavior in binary mixtures may be similar to that of PDPC ($T_m \leq -25$ °C). S_2 is, therefore, likely to be a reasonable approximation to the true solidus line for the DPPC/PDPC phase diagram. In any case, since S_1 and S_2 differ only slightly over the temperature range of the fluorescence measurements, calculations based on either solidus curve will exhibit only small differences.

Analysis of the Phase Diagram and Calculation of the Lateral Distribution of PnA Probes. Assuming solidus S_2,

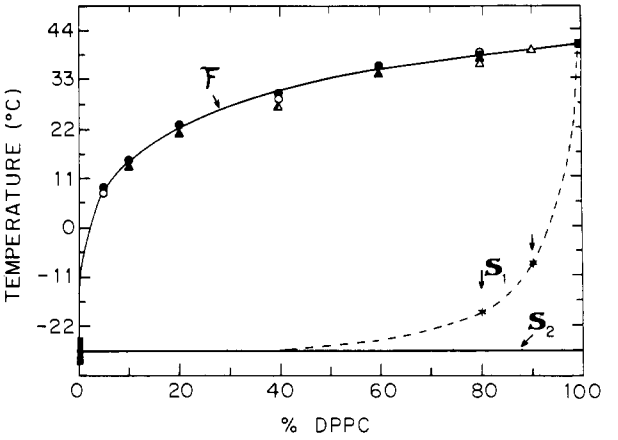

FIGURE 5: PDPC/DPPC phase diagram. The upper curve (F) represents the onset of lateral phase separation; temperatures determined from Figure 2 as described in the text. Filled circles are derived from *trans*-PnA (2C); open circles, *trans*-PnA-ME (2D); filled triangles, *cis*-PnA (2A); open triangles, *cis*-PnA-ME (2B). Curves S_1 and S_2 are discussed in the Results section. Arrows on S_1 represent highest possible temperatures at which the PDPC may be solid.

Table II shows the percent solid phase and the percent fluid phase in the DPPC/PDPC mixtures calculated as a function of temperature and composition of the mixture according to the lever rule (Moore, 1963; Lee, 1977). The data of Table II can be correlated with the results in Figures 2, 3, and 4. The low-temperature "leveling off" of the *cis*-PnA fluorescence parameters correspond to temperatures at which the solid phase comprises about 90% of the DPPC present, i.e., the completion of the lateral phase separation. For the trans probes, the "leveling off" temperatures of the polarization and quantum yield measurements represent solid phase formation comprising only 50–80% of the DPPC, the higher percentages for the smaller fractions of DPPC in the mixture.

The $K_p^{s/f}$ values are now readily calculated. The required parameters, the mole fraction of fluid (χ_f) and solid phase (χ_s), are obtained from Table II. The fractions of fluid phase probe (χ_f^p) and solid phase probe (χ_s^f) are contained implicity in eq 18 (using the fluorescence quantum yield measurements of Figure 4) and eq 21 (using the fluorescence polarization measurements of Figure 2). For temperatures below the lateral phase separation we calculate that $K_p^{s/f}$ for *cis*-PnA is 0.59 ± 0.12 (polarization) and 0.82 ± 0.33 (quantum yield); for *trans*-PnA, these values are 3.35 ± 0.65 (quantum yield) and 5.1 ± 1.2 (polarization). The results are in good agreement with the calculations based on absorption spectroscopy (Table

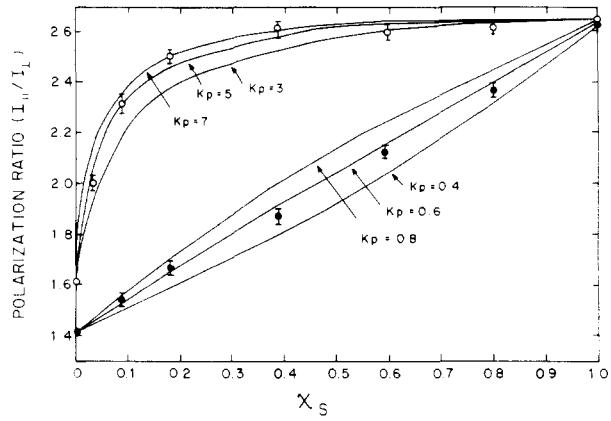

FIGURE 6: Fluorescence polarization vs. mole fraction of solid phase phospholipid (χ_s). The data points (○, *trans*-PnA; ●, *cis*-PnA) are derived from Figure 2 (0 °C) and Table II (0 °C). The smooth curves are calculated from eq 22 using several values of $K_p^{s/f}$ as shown in the figure. Values of the partial quantum yields at 0 °C are obtained from Figure 4. They are for *cis*-PnA: $Q_{\parallel}^{s} = 0.200$, $Q_{\perp}^{s} = 0.076$, $Q_{\parallel}^{f} = 0.061$, $Q_{\perp}^{f} = 0.043$; for *trans*-PnA: $Q_{\parallel}^{s} = 0.300$, $Q_{\perp}^{s} = 0.113$, $Q_{\parallel}^{f} = 0.044$, $Q_{\perp}^{f} = 0.027$.

I). The $K_p^{s/f}$ values calculated from fluorescence show no systematic temperature dependence.

These partitioning results may perhaps be better understood by comparison of the experimental polarization ratio values (as a function of the mole fraction solid phase) to values calculated from several $K_p^{s/f}$ values as shown in Figure 6, according to

$$\chi_s = \left[\frac{(Q_{\parallel}^{s} - PQ_{\perp}^{s})K_p^{s/f}}{PQ_{\perp}^{f} - Q_{\parallel}^{f}} + 1 \right]^{-1} \qquad (22)$$

Equation 22 is derived by rearranging eq 21 and substituting $\chi_s = 1 - \chi_f$. The experimental fluorescence values are those from 0 °C and details of the calculation are explained in the legend to Figure 6. It is apparent that the polarization values for *cis*-PnA approximate the curve for $K_p^{s/f} = 0.6$ and those for *trans*-PnA, although somewhat more scattered, approximate $K_p^{s/f} = 5$. The polarization of *cis*-PnA is nearly linear with χ_s, whereas the polarization of *trans*-PnA is highly nonlinear and responds most strikingly to χ_s below 0.25.

It is possible to construct the temperature dependence of the fluorescence polarization in mixtures of DPPC and PDPC using the calculated values of $K_p^{s/f}$ along with experimental values of the partial quantum yields of PnA probes in pure fluid PDPC and pure solid DPPC phases (see Figure 4). The results of such a calculation are shown and the method is explained in Figure 7. It is seen that the calculated temperature dependence of the polarization of *cis*-PnA (Figure 7) is quite similar to the observed behavior (Figure 2A).

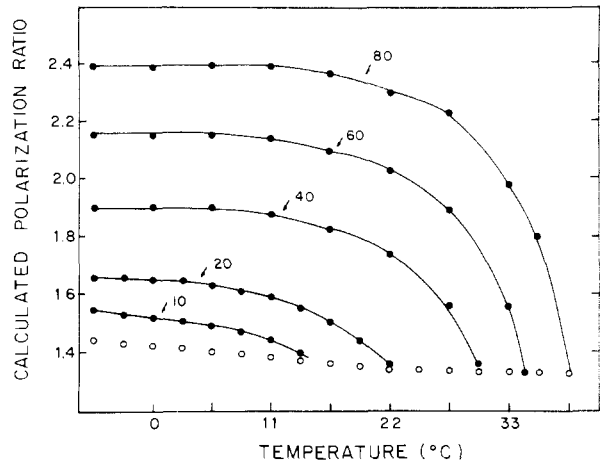

FIGURE 7: Calculated temperature dependence of *cis*-PnA fluorescence polarization in DPPC/PDPC mixtures. Curves are calculated according to a two step procedure; the numbers next to each curve represent the percent DPPC. (Step 1) For every temperature and every mixture, χ_s^{p} is calculated according to a rearrangement of eq 1, $\chi_s^{p} = [(1/K_p^{s/f})(\chi_f/(\chi_s) + 1)]^{-1}$ using a value of $K_p^{s/f} = 0.6$ and values of χ_s and χ_f from Table II. (Step 2) The polarization ratio is then calculated at each temperature for each mixture according to eq 19 using values of DPPC and PDPC partial quantum yields (Figure 4B) for *cis*-PnA. This treatment represents a simplification because the fluid phase composition changes as a function of temperature below the onset of the lateral phase separation and approaches a pure PDPC phase only at low temperatures where the lateral phase separation is complete. At higher temperatures, the fluid phase polarization and quantum yield values of mixtures are intermediate to DPPC fluid and PDPC fluid phase values. The open circles are experimental PDPC values. The filled circles are the calculated values for the mixtures.

Discussion

Distribution of the Geometrical Isomers of Parinaric Acid between Coexisting Solid and Fluid Phospholipid Phases. We have previously observed (Sklar et al., 1977b) that the transition temperature of several phospholipids appeared to be slightly higher when monitored with *trans*-PnA than with *cis*-PnA. In addition, when two phospholipid liposome populations were present, *trans*-PnA preferentially monitored the higher melting temperature component, whereas *cis*-PnA was sensitive to both components (Sklar et al., 1977b). These observations led us to hypothesize that *trans*-PnA preferentially partitions into solid phase phospholipids, while *cis*-PnA partitions more equally between coexisting phases. In this present paper we have used three spectroscopic parameters to quantitatively determine solid/fluid partition coefficients of the PnA molecules: the absorption spectrum, the temperature dependence of the fluorescence quantum yield, and the temperature dependence of the fluorescence polarization. In the mixed lipid system containing DPPC (as the solid component) and PDPC (as the fluid component) we conclude from all the spectral parameters that the solid/fluid partition coefficients ($K_p^{s/f}$) are 4 ± 1 for *trans*-PnA and 0.7 ± 0.2 for *cis*-PnA. Results obtained for the methyl ester derivatives of PnA indicate that their partitioning behavior is quite similar to that of the fatty acids (Figure 2). The factor which apparently governs the partition of the cis and trans probes is their molecular geometry. It seems reasonable to suggest that the extended or linear structure of the trans probes allows them to cocrystallize with solid lipid phases while the bent configuration of the cis probes apparently causes them to be relatively excluded from solid phases. We view the conjugated tetraene chromophore as relatively rigid in comparison to either the melted saturated chains or the nonconjugated polyunsaturated chains which have considerable flexibility.

Structural Order Persists above Phospholipid Transition Temperatures. A persistence of order, "clustering", has been identified in phosphatidylcholines containing unsaturated acyl chains at temperatures above the gel to liquid crystalline transition temperature (Lee et al., 1974; Wu & McConnell, 1975). In PDPC, we observe an elevation of the fluorescence polarization ratio which persists to near 0 °C, an estimated 25–30 °C above the transition temperature (Figure 3) which may result from cluster formation. We observe also in our DPPC and its mixtures a "tail", particularly conspicuous in the fluorescence properties of the trans probes, beginning at temperatures from 5–10 °C above the transition temperature.

This tail is similar in magnitude to the phase separation in the 5% DPPC mixture which contains 3% solid DPPC at 0 °C (Table II). The commercial DPPC sample used in these determinations contains 1% stearoyl chains (i.e., 2 mol % of the PC molecules contain stearoyl chains). The tail observed with the trans probes may reflect clustering, particularly of those molecules containing stearoyl chains. The elevated polarization, quantum yield, and persistent long-lifetime component observed slightly above the DPPC transition (Sklar et al., 1977b) are consistent with the "cluster" as a locally ordered environment comparable to a phospholipid solid phase. Minimally, the cluster might be a ring of acyl chains ordered over a time scale long compared to the *trans*-PnA fluorescence lifetime (about 20 ns at 41 °C in DPPC). This duration, 100 ns or longer, is comparable to the jump–diffusion time of phospholipids, suggesting that the cluster lifetime may be governed by the diffusion of phospholipids rather than the more rapid trans-gauche isomerization of the acyl chains. It is probable that the same factors which enhance the sensitivity of *trans*-PnA to solid lipid make it sensitive to clusters.[8]

Relative Sensitivity of Quantum Yields and Polarization to Phospholipid Structural Reorganization. We have previously suggested that the temperature dependence of the fluorescence quantum yield was linear in a log Q vs. $1/T$ plot for PnA molecules in solvent, pure fluid lipid, or pure solid lipid (Sklar et al., 1977a,b). As seen in Figure 4, the linear dependence is only a reasonable approximation. As solid phase phospholipids are cooled, the probe quantum yield does not increase exponentially indefinitely. We caution other investigators against interpreting this flattening at low temperature in terms of additional reorganization.

Due to its preferential association with solid phase and enhanced quantum yield in phospholipid solid phase, *trans*-PnA is ~25 times more sensitive to solid DPPC than fluid PDPC and is particularly sensitive to the first formed solid. In contrast, the fluorescence parameters of *cis*-PnA reflect these phases more proportionately, and it is quite difficult to detect a lateral phase separation in mixtures containing a few percent solid phase with *cis*-PnA quantum yield measurements. Since $K_p^{s/f}$ for *cis*-PnA is near 1, measurements of the polarization of fluorescence of *cis*-PnA tend to reflect the true temperature range of, and the fraction of lipids involved in, a phospholipid lateral phase separation.

Motion of PnA Probes in Phospholipid Membranes. An analysis of the motion of PnA probes is important because these motions probably reflect segmental or "wobbling" motions of the membrane acyl chains (see Kinoshita et al., 1977; Dale et al., 1977). Since the fluorescence lifetimes of these molecules are strongly dependent upon temperature and environment (Sklar et al., 1977a,b), the weak temperature dependence of the polarization of the cis probes in the fluid phase probably reflects a compensation of motional variation by fluorescence lifetime variation (see Lentz et al., 1976a,b). The nearly limiting solid phase polarization values probably reflect extreme immobilization of acyl chains on a time scale at least 100–1000 ns.

[8] *trans*-PnA may cluster when present as a large proportion of the lipids (Sklar and Blanchard, unpublished result). Clusters are inferred from an excitonic absorption shift (similar to that shown in Figure 1B) increasing with the mole fraction of *trans*-PnA. We estimate that there is less than 5% *trans*-PnA cluster at 1 *trans*-PnA/100 phospholipids and 50% cluster when the ratio is 1 *trans*-PnA/10 phospholipids. A plot of our data similar to that described for spin labels (Rey & McConnell, 1977) suggests the *trans*-PnA cluster is a trimer. All of the data presented in this paper are from samples containing approximately 1 PnA/166 phospholipids where PnA clustering is undetectable.

A qualitative comparison of the motion of these probes can be made from the static polarization measurements presented here. In phospholipid fluid phase these trends are apparent: the trans probes exhibit higher polarization than the cis probes; the fatty acid probes exhibit higher polarization than the methyl ester probes; polarization ratios are significantly higher in the DPPC fluid phase than in the PDPC fluid phase at the same temperature. In principle, an increased polarization ratio can arise from either reduced probe motion or reduced fluorescence lifetime. Since fluorescence lifetimes for these chromophores vary with quantum yield (Sklar et al., 1977a,b), much of the polarization differences may be related to motional differences. We suggest therefore, that the lower polarization of the methyl esters indicates increased motional freedom: the fatty acid carboxyl group may anchor PnA at the membrane–water interface, and the less polar ester may penetrate more deeply into the fluid bilayer interior. The consistently higher fluid phase polarization of the trans probes compared to that of the cis probes may reflect motional freedom around the long axis of the membrane acyl chains; such a rotation would lower the polarization of the cis probes only. Finally, it appears that at a given temperature, probe motion is greater (either more rapid or wider angle) in PDPC than DPPC. This seems reasonable in view of PDPC being much farther above its transition temperature.

Relevance of the DPPC/PDPC Phase Diagram to the Structure of Visual Photoreceptor Membranes. The phospholipids of the inner monolayer of the bovine retinal rod outer segment membranes are predominantly phosphatidylcholine (Smith et al., 1977; Miljanich, Nemes, and Dratz, unpublished experiments) occurring as three classes: disaturated PC (particularly DPPC, ~20%), saturated–polyunsaturated PC (such as PDPC, ~50%), and dipolyunsaturated PC (~25%) (Miljanich et al., 1979). Thermal transitions in isolated rod PC occur over a temperature range very similar to that observed here for the 20% DPPC/PDPC mixture (Sklar et al., 1979; Miljanich et al., 1978, 1979). A degree of order appears to persist near physiological temperatures.

Specific lipid composition may provide lateral compressibility in membranes (Linden et al., 1973) which may accommodate protein structural changes. It may be relevant in this regard that rhodopsin appears to change the volume of the disk membrane upon light excitation (Lamola et al., 1974). It is conceivable that phase boundaries could be involved in regulating the permeability of these membranes (Trauble & Eibl, 1975). The possible effect of cholesterol, which comprises 10 mol % of the membrane lipids is considered elsewhere (Sklar et al., 1979).

Conclusion

cis-PnA and *trans*-PnA are a unique pair of fluorescent membrane probe molecules which preferentially partition into fluid and solid lipid domains, respectively. Any analysis of the structure of biological membranes or synthetic lipid bilayers using these probes must take into consideration their partitioning among coexisting phases. *trans*-PnA is sensitive to a few percent solid lipid but is relatively insensitive to the formation of solid lipid in excess of 50%. Thus, the fluorescence behavior (quantum yield or polarization) of this probe is nonlinearly related to the relative amounts of solid and fluid phases present (Figure 6). *cis*-PnA, however, has only a slight preference for fluid phase and its fluorescent behavior is nearly linearly correlated with the amount of solid and fluid phases (Figure 6). Used in tandem, these two probes should allow an accurate index of membrane lipid structural reorganization.

The DPPC/PDPC phase diagram constructed from fluorescence data exhibits solid phase immiscibility, presumably due to the large differences in the transition temperatures of the components. This phase behavior resembles that observed for other binary mixtures of lipids with similar large differences in transition temperatures.

Structural changes are observed in PDPC and possibly DPPC and their mixtures, above their transition temperatures. This behavior is ascribed to the presence of ordered lipid "clusters" in the bulk fluid phase.

Added in Proof

The partition of fatty acids between water and hexane is concentration dependent (Smith & Tanford, 1973). Therefore the lipid–water K_p values for PnA probes are valid only for the specific experimental conditions described. Preliminary experiments (L. A. Sklar, unpublished experiments) indicate that a tenfold decrease in PnA concentration results in less than a twofold increase in K_p. Since all experiments described here were performed within a narrow PnA concentration range, our conclusions are not affected.

Acknowledgments

The authors thank Cathy Arocha and Kaye Shewmaker for assistance in the preparation of the manuscript. L.A.S. acknowledges the encouragement and support of Dr. Henry Pownall during the final stages of manuscript preparation. While this manuscript was being completed, we became aware of another treatment of probe partitioning (Foster & Yguerabide, 1979) and were kindly provided with a preprint by Dr. J. Yguerabide.

References

Azumi, T., & McGlynn, S. (1962) *J. Chem. Phys. 37*, 2413.
Chen, P. S., Toribura, T. Y., & Warner, H. (1956) *Anal. Chem, 28*, 11.
Chen, R. F., & Bowman, R. L. (1965) *Science 147*, 729.
Dale, R. E., Chen, L. A., & Brand, L. (1977) *J. Biol. Chem. 252*, 7500.
Foster, M., & Yguerabide, J. (1979) *J. Membr. Biol.* (in press).
Jacobs, R. E., Hudson, B. S., & Andersen, H. C. (1977) *Biochemistry 16*, 4349.
Kinoshita, K., Kawato, S., & Ikegami, A. (1977) *Biophys. J. 20*, 289.
Lamola, A. A., Yamane, T., & Zipp, A. (1974) *Biochemistry 13*, 738.
Lee, A. G. (1977) *Biochim. Biophys. Acta 472*, 285.
Lee, A. G., Birdsall, N. J. M., Metcalf, J. C., Toon, P. A., & Warren, G. B. (1974) *Biochemistry 13*, 3699.
Lentz, B. R., Barenholz, Y., & Thompson, T. E. (1976a) *Biochemistry 15*, 4521.
Lentz, B. R., Barenholz, Y., & Thompson, T. E. (1976b) *Biochemistry 15*, 4529.
Linden, C. D., Wright, K., McConnell, H. M., & Fox, C. F. (1973) *Proc. Natl. Acad. Sci. U.S.A. 70*, 2271.
Mabrey, S., & Sturtevant, J. (1976) *Proc. Natl. Acad. Sci. U.S.A. 73*, 3862.
Miljanich, G. P., Mabrey, S. V., Brown, M. F., Sturtevant, J. M., & Dratz, E. A. (1978) *Biophys. J. 21*, 135a.
Miljanich, G. P., Sklar, L. A., White, D. L., & Dratz, E. A. (1979) *Biochim. Biophys. Acta* (in press).
Moore, W. J. (1963) in *Physical Chemistry*, p 128, Prentice-Hall, Englewood Cliffs, NJ.
Phillips, M. C., Ladbrooke, B. D., & Chapman, D. (1970) *Biochim. Biophys. Acta 196*, 35.
Raubach, R. A., Franklin, L. K., & Dratz, E. A. (1974) *Vision Res. 14*, 335.
Rey, P., & McConnell, H. M. (1977) *J. Am. Chem. Soc. 99*, 1637.
Shimshick, E. J., & McConnell, H. M. (1973) *Biochemistry 12*, 2351.
Shinitzky, M., Dianoux, A.-C., Gitler, C., & Weber, G. (1971) *Biochemistry 10*, 2106.
Simon, S. A., Stone, W. L., & Busto-Lattore, P. (1977) *Biochim. Biophys. Acta 468*, 378.
Sklar, L. A., Hudson, B. S., & Simoni, R. D. (1975) *Proc. Natl. Acad. Sci. U.S.A. 72*, 1649.
Sklar, L. A., Hudson, B. S., Peterson, M., & Diamond, J. (1977a) *Biochemistry 16*, 813.
Sklar, L. A., Hudson, B. S., & Simoni, R. D. (1977b) *Biochemistry 16*, 819.
Sklar, L. A., Miljanich, G. P., Bursten, S. L., & Dratz, E. A. (1979) *J. Biol. Chem.* (in press).
Smith, R., & Tanford, C. (1973) *Proc. Natl. Acad. Sci. U.S.A. 70*, 289.
Smith, H. G., Fager, R. S., & Litman, B. J. (1977) *Biochemistry 16*, 1399–1405.
Trauble, H., & Eibl, H. (1975) in *Functional Linkage in Biomolecular Systems* (Schmitt, F. O., Schneider, D. M., & Crooouthers, D. M., Eds.) pp 59, Raven Press, New York, NY.
Weber, G. (1952) *Biochem. J. 51*, 145.
Wu, S. H.-W., & McConnell, H. M. (1975) *Biochemistry 14*, 847.